Available online at www.sciencedirect.com

SciVerse ScienceDirect

journal homepage: http://www.elsevier.com/locate/rpor

Original research article

Technical and dosimetric aspects of the total skin electron beam technique implemented at Heidelberg University Hospital

Frank W. Hensley[a,*], *Gerald Major*[a], *Carolin Edel*[b], *Henrik Hauswald*[a], *Marc Bischof*[a]

[a] *Department of Radiation Oncology, University Hospital Heidelberg, Im Neuenheimer Feld 400, 69120 Heidelberg, Germany*

[b] *Department of Radiation Protection, Zentralbereich Neuenheimer Feld, University of Heidelberg, Im Neuenheimer Feld 327, 69120 Heidelberg, Germany*

ARTICLE INFO

Article history:
Received 6 May 2013
Accepted 4 July 2013

Keywords:
Total skin therapy
Electrons
Dosimetry
X-ray contamination

ABSTRACT

Aim: To give a technical description and present the dosimetric proporties of the total skin electron beam technique implemented at Heidelberg University Hospital.

Background: Techniques used for total skin electron beam irradiation were developed as early as in the 1960s to 1980s and have, since then, hardly changed. However, new measurements of the established methods allow deeper insight into the dose distributions and reasons for possible deviations from uniform dose.

Materials and methods: The TSEI technique applied at Heidelberg University Hospital since 1992 consists of irradiating the patient with a superposition of two beams of low energy electrons at gantry angles of 72° and 108° while he is rotating in a standing position on a turntable at 370 cm distance from the accelerator. The energy of the electron beam is degraded to 3.9 MeV by passing through an attenuator of 6 mm of Perspex. A recent re-measurement of the dose distribution is presented using modern dosimetry tools like a linear array of ionization chambers in combination with established methods like thermoluminescent detectors and film dosimetry.

Results: The measurements show a strong dependence of dose uniformity on details of the setup like gantry angles.

Conclusions: Dose uniformity of −4/+8% to the majority of the patient's skin can be achieved, however, for the described rotational technique overdoses up to more than 20% in small regions seem unavoidable.

* *Corresponding author*. Tel.: +49 6221 56 37666; fax: +49 6221 56 7222.
E-mail addresses: frank_hensley@med.uni-heidelberg.de, frank.hensley@gmx.de (F.W. Hensley).

1507-1367/$ – see front matter © 2013 Greater Poland Cancer Centre. Published by Elsevier Urban & Partner Sp. z o.o. All rights reserved.
http://dx.doi.org/10.1016/j.rpor.2013.07.002

1. Background

Total skin electron irradiation (TSEI) is a radiotherapy technique used in the treatment of a number of malignant diseases occurring in the skin such as mycosis fungoides, Sézary syndrome or Kaposi's sarcoma.[1–9] TSEI has shown good and even excellent results in experiences observed over many years[2,3,5,6] with long term control of early staged disease,[2,3,5,6] and also satisfactory palliative results.[2,8,9] These diseases can affect large areas or even the total surface of the skin so that the target in radiotherapy may be equally large. Doses required for the treatment of cutaneous lymphoma are in the region of 30–36 Gy[1,4,5] although experiences with lower doses of 10–20 Gy are discussed.[5,6] Generally, radiotherapy is performed with low energy electrons with a penetration of less than 1–2 cm which exclude other organs at risk than the skin itself. The tolerance dose of healthy skin is around 50 Gy,[10] so that the risk of therapeutic doses around 36 Gy is acceptable, except for the eye lens and toe- and fingernails which can be excluded by additional shielding during treatment.

Treating the entire skin of an adult human with his arms stretched overhead requires a sufficiently uniform radiation field of around 50 cm × 220 cm. Physical conditions for large area electron treatment have been described in literature.[11–13] Techniques to produce large electron fields include the superposition of two fields at two gantry angles,[11–16] matching multiple fields,[3,17] producing single large fields with a special beam flattening filter,[18] using multiple rotational arc fields[19] or by movement of the patient through a shorter field on a translation couch.[20] Treating the complete circumference of the patient is achieved by either irradiating the patient with static fields from various directions (which requires different positioning of the patient for each field)[11,12,16] or by rotating the patient in the beam.[14,15,18] The technique used at Heidelberg University Hospital was developed in 1992 and applies a combination of the methods described by AAPM Rept. 23.[12] and Müller-Sievers et al.[14,15]. Aim: This work reports a recent remeasurement of the Heidelberg set-up for total skin electron beam therapy which was necessary after a software upgrade of the accelerator which caused a reduction of the applicable field size.

2. Materials and methods

2.1. *Patient set-up for TSEI*

TSEI at Heidelberg Department of Radiation Oncology is applied with a Siemens Oncor accelerator by rotating the standing patient in a superposition of two large fields of low energy electrons at gantry angles of 72° and 108° (Fig. 1). The patient stands on a turntable with axis of rotation at 370 cm distance from the accelerator focus. The patient holds a swivel bar to keep his arms stretched and to support his stand. To help weak patients stand during the long treatment times of around 30 min, the patients can optionally lean against a bicycle seat mounted on a post behind the patient.

During rotational irradiation, parts of the inner leg of the patient are shielded by the other leg. To reduce this effect, the patient stands in two swordsman-like positions, alternating the extended leg each day (Fig. 2). Remaining areas of skin which show insufficient reaction to the radiation are boosted with single fields of low energy electrons at clinical decision.

The motion of the turntable is initiated by the "beam on" signal of the accelerator and stopped on "beam off". Turntable motion is controlled by a photoelectric sensor which sends a signal to the accelerator to interrupt the irradiation, should the rotation stop. An electronic counter displays the number of rotations with a resolution of 1/10th. To ensure a minimum of beam overlap, the position at which irradiation stops at each fraction is noted, and the next fraction is started at this position.

Treating the entire skin of an adult human with his arms stretched overhead requires a sufficiently homogeneous radiation field of around 50 cm × 220 cm. The maximum collimator setting for electrons that can be run in patient mode by the accelerator Siemens Oncor is 33 cm × 33 cm at 1 m, produced

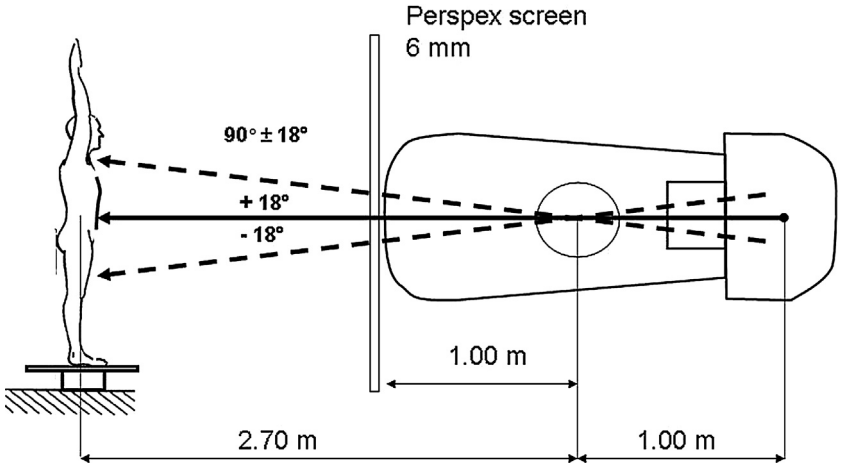

Fig. 1 – Patient setup for total skin electron beam irradiation (TSEI) at Heidelberg University Hospital. The patient stands on a rotating turntable at 3.70 m distance from the accelerator focus and is irradiated by two large superposed electron beams at gantry angles of 70° and 110°. The 6 MeV electrons from the accelerator are attenuated by a screen of 6 mm Perspex to an incident energy of 3.9 MeV at the patient.

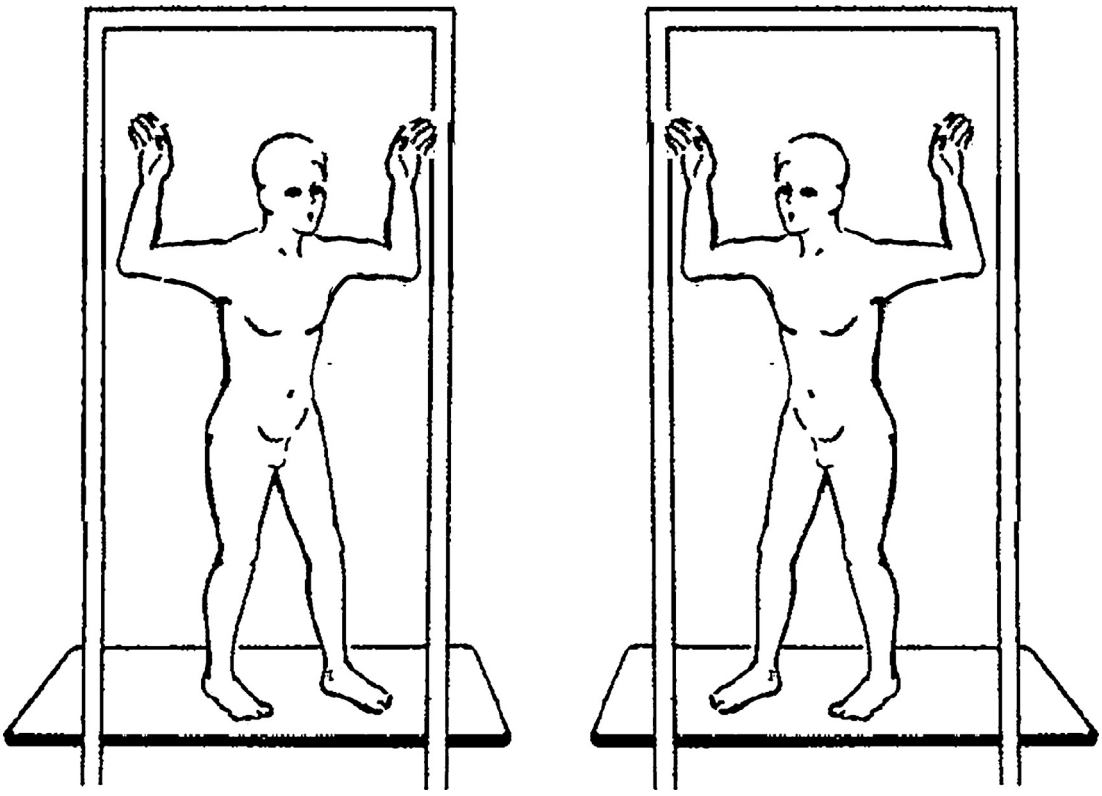

Fig. 2 – Alternating patient position with each fraction to reduce shielding of the inner side of the legs. Modification of figure from AAPM Report TG 23,[12] with permission of AAPM publishing.

by programming the accelerator for a 25 cm × 25 cm electron applicator and 6 MeV electrons, and then irradiating without applicator. Irradiation is therefore performed without the additional collimation and flattening by the applicator. This produces a field defined by the setting of the collimator jaws to 33cm × 33 cm at 1 m which projects to 122 cm × 122 cm at 370 cm. To homogeneously cover the required field length of 220 cm with dose, two inclined fields with gantry angles of 72° and 108° (90 ± 18°) are superposed. The required electron penetration of a few mm is given for electrons of around 4 MeV. To arrive at this energy, the 6 MeV electrons of the accelerator are attenuated to 3.9 MeV by a screen of 6 mm of Perspex (plus the additional air column of 270 cm) placed between the accelerator and the patient at 200 cm distance from the focus.

2.2. *Dosimetry for rotational treatment with superposed fields*

To determine the optimal inclination for the superposed fields, first the profile of a single beam at gantry angle 90° is measured at the distance of the rotation axis. The measured profile data is fed into a spreadsheet programme with which the superposition of two beams at variable inclination angles can be calculated. The calculation uses a simplified geometry shown in Fig. 3. From these calculations optimal beam combinations are selected which predict homogeneous dose along a sufficient length. The superposition of two inclined beams is then measured with integrating dosimeters for selected gantry angles and examined for sufficient homogeneity. All measurements are made on the rotation axis of the turntable at 370 cm distance from focus, and including the 6 mm Perspex sheet which was positioned 270 cm from focus.

The measurements of the single profile at 90° and the superposed fields were performed with a linear ionization chamber array (LA48, PTW-Freiburg, Lörracher Str. 7, Freiburg, Germany) which was mounted on a plank positioned at the rotation axis. The array consists of 47 sealed ionization chambers (dimensions 4 mm diameter × 0.5 mm depth) arranged in a straight row at distances of 8 mm thus allowing simultaneous measurement along a length of 368 mm. Each chamber has a sensitive volume 0.008 cm^3 filled with liquid iso-octane. The chamber signals were read with a PTW Multidos electrometer, and directly fed into Excel spreadsheets with the PTW software DosiCom (all PTW-Freiburg). The entrance plane of the array was covered by 1 mm of water equivalent plastic (RW3, PTW-Freiburg, density 1.045 g/cm^3) resulting in an effective depth of measurement of 1.8 mm (effective depth of measurement for the LA48 detectors: 0.75 mm). To detect low energy radiation (which would produce only superficial dose), a second set of measurements was performed without the plastic. A series of measurements were made with the centre of the 48 cm long array at 6 positions of increasing height above the surface of the turntable covering the complete length from the turntable to the ceiling (255 cm). At each position, measurements were made for gantry angles of 90°, 68°, 70°, 72°, 78°, 102°, 108°, 110°, and 112°. The profile segments at the 6 positions were then arranged in sequence, resulting in composed profiles of 223.8 cm length. Superposed fields at gantry

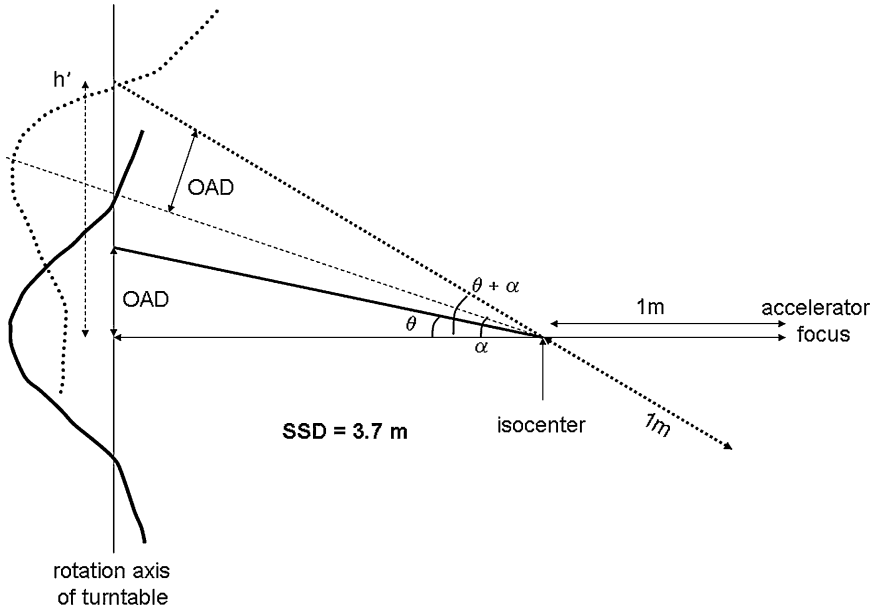

Fig. 3 – Geometry used to calculate supposed beams. The line connecting any point in the profile with the isocenter is rotated by the beam inclination angle α. The new line's intersection with the rotation axis of the turntable is considered as the new position of the point. The source surface distance (SSD) of any point in the profile is approximated by its distance to the isocenter plus 1 m. The inverse square of the approximated SSD is used to correct the dose for distance.

angles of $90 \pm 20^\circ$ and $\pm 18^\circ$, and for comparison at $90 \pm 22^\circ$ and $90 \pm 12^\circ$ were simulated by summation of the profiles at the two respective angles.[1]

For the chosen field combination of $90 \pm 18^\circ$ the dose for a given monitor setting (5000 MU) on an anthropomorphic phantom rotating on the turntable in patient position was measured. Dose was measured with LiF thermoluminescent detectors (TLDs) at various ventral, dorsal and sideward positions on the rump, neck, head, arms and legs phantom shown in Fig. 4. The results of these measurements are used to examine the dose homogeneity produced under rotation in a realistic geometry. The mean dose on the trunk of the phantom is used to calculate the monitor setting per Gy of prescribed dose. This setting is then applied as standard to all following patients. During the first patient fractions, it is verified by TLD measurements and, if necessary, corrected.

Depth dose curves of the resulting superposed fields were measured by irradiating a sheet of ready-packed radiographic film (Kodak X-OMAT V, Eastman Kodak, Rochester, NY, USA) between the slabs of a rotating anthropomorphic phantom (Alderson Rando Phantom, Alderson Research Laboratories, Inc., Stamford, CT, USA). The edge of the light tight envelope was folded in on one side of the film to form a minimal overlap. This side was placed flush with the ventral surface of the phantom, and at this position of the exposed film the depth curve was measured. A dose calibration curve for the films was measured for 8 MeV electrons at 20 mm depth where the mean electron energy is 4 MeV. Films were scanned with a Vidar scanner (Vidar Dosimetry Pro Advantage, VIDAR Systems Corporation, 365 Herndon Parkway, Herndon, VA, USA) and analyzed with the beam analysis software PTW Mc^2 (PTW-Freiburg).

3. Results

Fig. 5 shows profiles at 370 cm and gantry angle 90° of a 6 MeV electron field collimated to 33 cm × 33 cm at 1 m and degraded by 6 mm of Perspex. The lower profile is measured without, the higher profile with 1 mm of additional material on the entrance window of the linear array; both are normalized at the maximum of the lower curve. The additional material apparently leads to a dose "build up" of 4% at the maximum (central axis) of the profile which decreases towards the field edges. The profiles have bell shape with a half-width of 156 cm. The dose variation within 30 cm distance from central axis is 10%. This variation defines the lateral homogeneity of the beams in patient treatments. The profiles are slightly asymmetrical with higher dose on the side facing towards the turntable. The higher dose most probably is caused by scatter radiation from the turntable and the floor.

Fig. 6 shows the long profiles of two beams superposed at gantry angles of $90 \pm 12^\circ$, $90 \pm 18^\circ$, $90 \pm 20^\circ$ and $90 \pm 22^\circ$. All profiles are normalized at the height of the isocenter (111.3 cm above the surface of the turntable) and show the effect of gantry angle on the homogeneity of the superposed profile.

[1] A second set of measurements of both the single profile at 90° gantry angle and the superposed fields was performed with radiochromic films (Gafchromic EBT3, International Speciality Products, Inc., 1361 Alps Road, Wayne, NJ, USA) and analyzed with a Microtek ScanMaker 1000XL flatbed scanner (Microtek International, Inc., No. 6 Industry East Road 3, Science-based Industrial Park, Hsinchu, Taiwan). These measurements yielded identical results as the array measurements (apart from some scanner artefacts), and are therefore not shown in this publication.

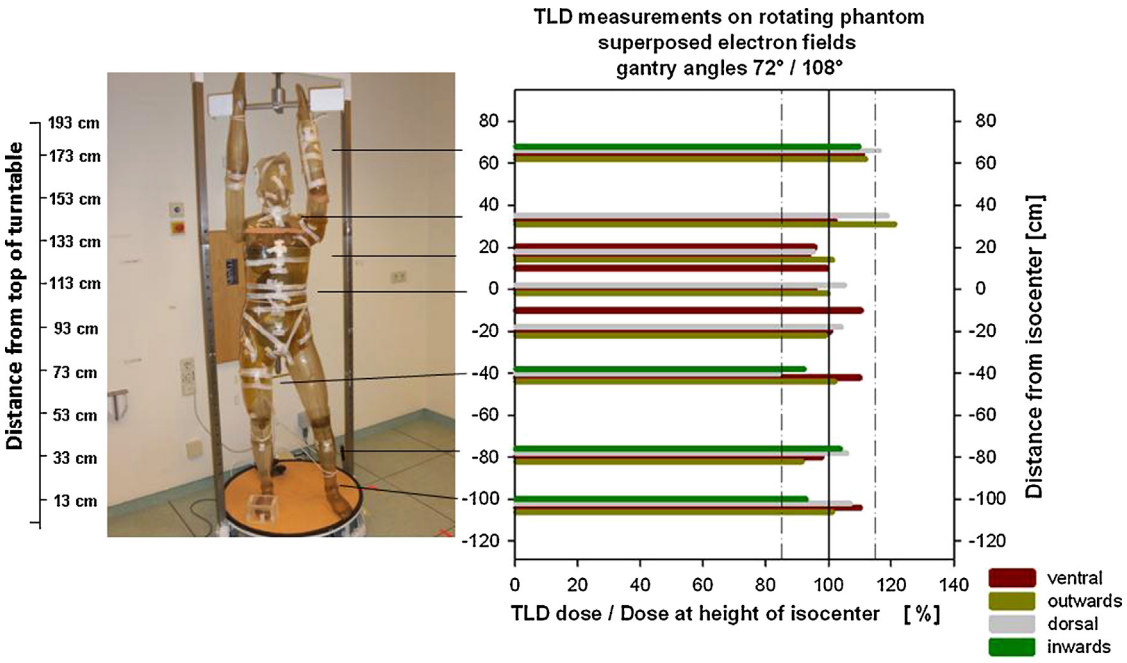

Fig. 4 – (Left side) Set-up for TLD measurements of the dose distribution on an anthropomorphic phantom rotating in two superposed electron beams at gantry angles 90 ± 18°. (Right side) Results of the TLD measurements on the anthropomorphic phantom. The data are plotted against the height in which they were measured and normalized at the height of the isocenter where dose is prescribed. The horizontal connecting lines show the position on the phantom in which the dose was measured. At several positions, dose was measured at the ventral, lateral (outward) and dorsal side of the phantom. Dose was measured on both legs of the phantom at lateral inward and outward positions to test the effect of mutual shielding by the other leg. On the motionless phantom, no effect of shielding was observed.

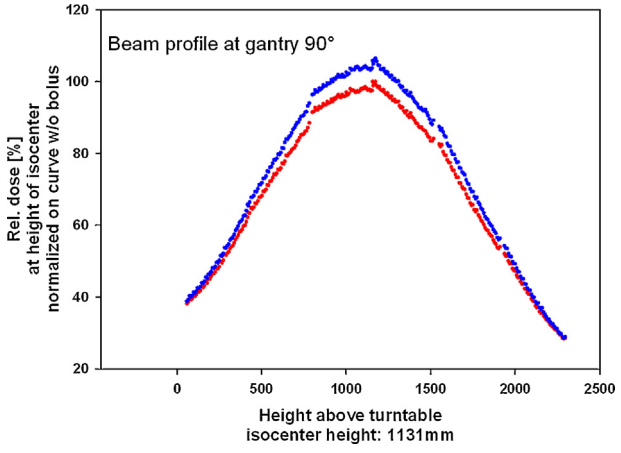

Fig. 5 – Profile of a single electron beam at 370 cm and gantry angle 90° of a 6 MeV electron field collimated to 33 cm × 33 cm at 1 m and degraded by 6 mm of Perspex. The higher curve was measured using an additional bolus of 1 mm of tissue equivalent material in front of the detector and shows a build up dose of 4% at the central axis which decreases towards the field edges. Both curves are normalized to the dose in the lower profile (without bolus) at the beam axis (=height of isocenter).

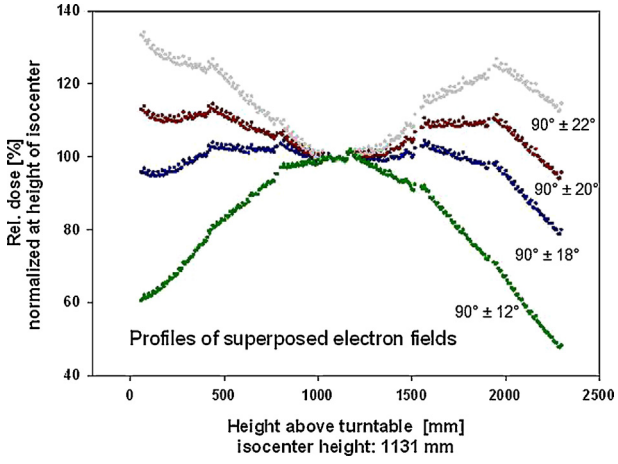

Fig. 6 – Profiles along the long axis of the dose distribution generated by two electron beams superposed at gantry angles of 90 ± 12°, 90 ± 18°, 90 ± 20° and 90 ± 22°. All profiles are normalized at the height of the isocenter (1113 mm above the surface of the turntable). The data show the effect of gantry angle on the homogeneity of the superposed profile.

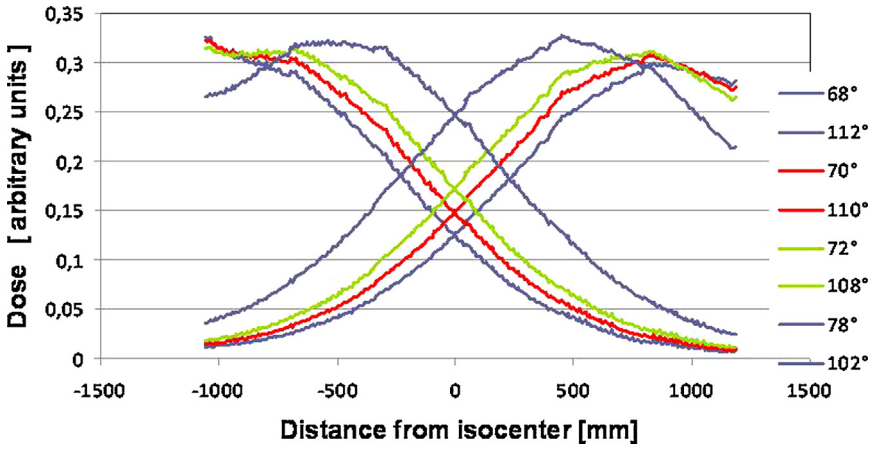

Fig. 7 – Measured profiles of the single beams at gantry angles of 68°, 70°, 72°, 78°, 102°, 108°, 110° and 112°. In the region between the top of the turntable and 250 cm height, only half of the profile contributes to the dose in the measured area.

The profiles at $90 \pm 18^{\circ}$and $90 \pm 20^{\circ}$show a homogeneity of around ±10% reaching from the surface of the turntable to a height of 220 cm.The superposition at $90 \pm 18^{\circ}$ was selected fur the further investigations (and for patient treatments) since it shows the lowest dose variation of ± 4% (difference from the normalization dose at height of isocenter) in the region between 0 and 200 cm height. For smaller and larger superposition angles, one can see increasing dose inhomogeneity towards the profile ends.

Fig. 7 shows the profiles of the single beams measured at the same gantry angles of 90° and also normalized at height of isocenter. Obviously, for the chosen angles, only about half the beam profile contributes to the dose in the area of interest to treat a patient. Also here, the differences between the profile shapes of the lower and higher beams show the presence of additional scatter from the floor.

In Fig. 8 the calculated superposed fields are shown together with the measured superpositions. At the lower end of the profiles, the measured profiles generally show higher doses than the calculation due to scatter dose from the floor. This effect increases with larger angles of inclination, i.e. when the lower beam is directed steeper towards the floor.

Fig. 4 shows the results of the TLD measurements on the anthropomorphic phantom. For comparison of dose deviations, a mean dose at the phantom trunk is calculated. This dose is also used as reference dose to calculate monitor units. At positions along the trunk of the phantom, measured dose is constant within −6/+10% of the mean dose. Larger dose deviations were measured at the neck, head, arms and legs of the phantom. At the arm of the phantom (175 cm above turntable) and at the shins (31 cm above turntable) doses of up to 123% were measured. At positions on the neck and head (146/165 cm above turntable) doses of up to 127% (dorsal neck) and 132% (lateral head) of mean dose were measured.

From the TLD measurements along the phantom trunk a standard monitor preset for 1 Gy at the trunk surface was calculated.

The depth dose curve (Fig. 9) measured in the rotating phantom shows that the resulting electron spectrum has a most probable energy at the surface of 3.9 MeV (mean energy 2.6 MeV). The surface dose (at 0.5 mm depth) is 89%, the maximum of the depth dose curve lies at 2 mm and the depth of 80% of maximum dose is 6.6 mm. Practical range of the electrons is 18 mm. The curve shows an X-ray background of 1.2%.

4. Discussion

Measured and calculated profiles of the superposed beams show a number of differences that are not reflected by the calculations: the measured profiles show higher dose at their lower end due to scatter radiation from the floor. This scatter radiation is already visible in the asymmetric shape of the profile at 90°, and increases with the inclination of the beam. It is therefore an additional effect of previously unknown size which cannot readily be included in the calculations. A similar finding is reported by Antolek and Hogstrom who use Fermi Eyges theory of multiple electron scattering to model the profiles of two overlaid beams but also do not model floor scattering.[21] The dose of the inclined beam is corrected by the inverse square of the point's distance to the accelerator focus. This correction is most probably incorrect because the Perspex beam degrader acts as a secondary source from which a new distance dependence is initiated. Due to the large extension of this secondary source the dose from radiation originating here will probably not follow an inverse square law but some lower potential of distance from some virtual source at a shorter distance from the point. Additionally, the position of the virtual source will probably vary with the off-axis distance of the considered point due to different absorption and scattering of electrons passing through the Perspex plate at different angles. Considering these principle deficiencies of the calculation method, the measured and calculated profiles shown in Fig. 8 show an unexpectedly good agreement. In summary, the described simple method of calculation is sufficient to estimate useful angles for beam superposition.

The position and width of narrow profiles of the single inclined beams shown in Fig. 7 are an important reason for the strong dependence of the superposed profile on beam angle. Using a larger field of electrons would most probably reduce

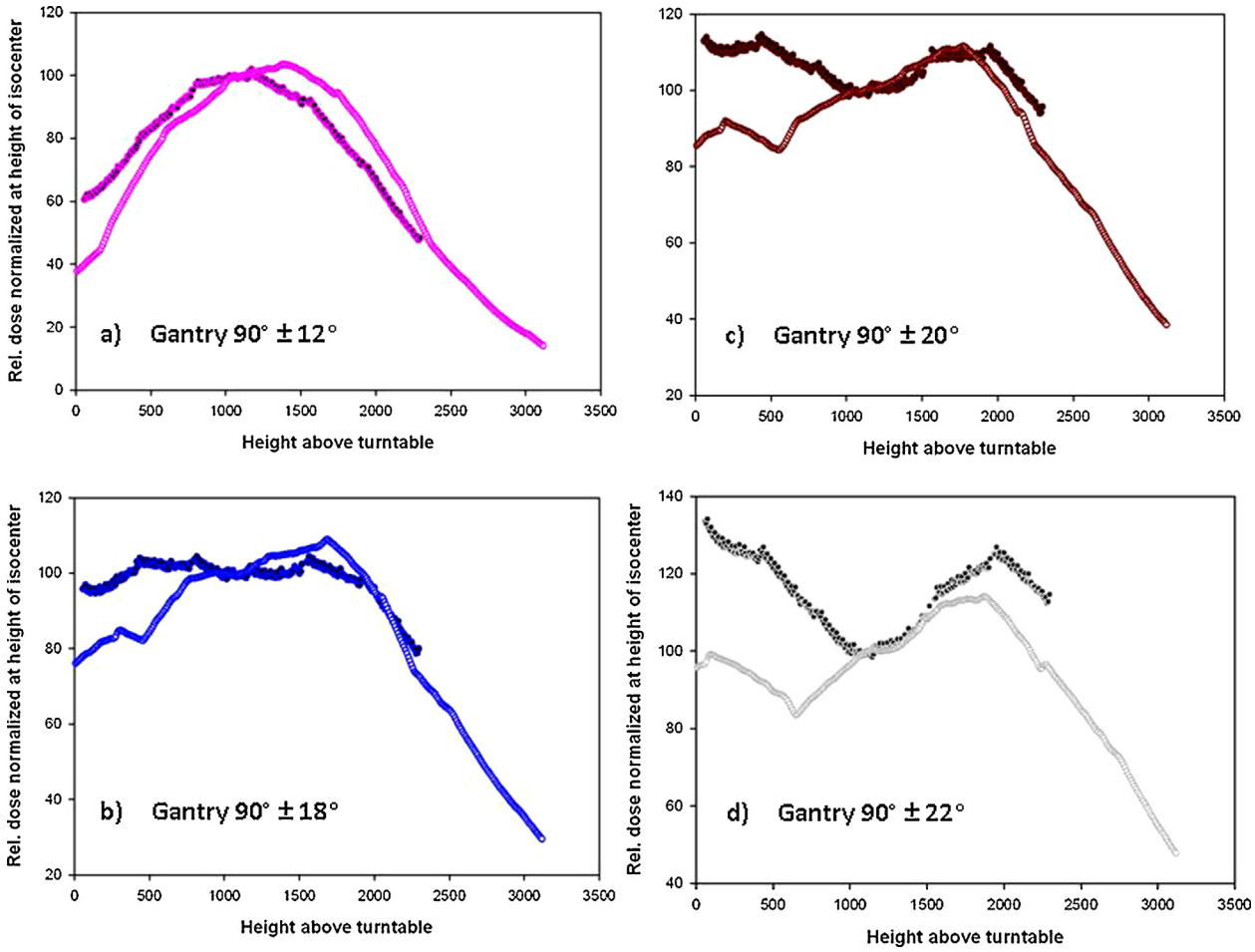

Fig. 8 – Comparison of calculated and measured superpositions of two beams with inclination angles of (a) 90 ± 12°, (b) 90 ± 18°, (c) 90 ± 20° and (d) 90 ± 22°. (Measured profiles: full circles, calculated profiles: open circles.) Towards the surface of the turntable, the measured profiles show a higher dose, probably from floor scatter which can be not predicted by the simple calculations. This scatter component increases with growing inclination of the beam.

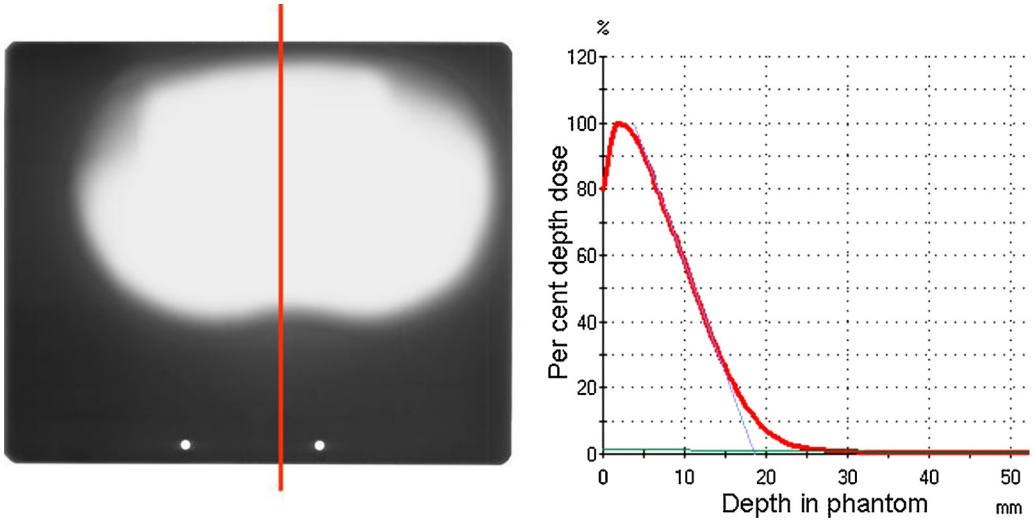

Fig. 9 – (Left side) Radiographic film exposed between the slabs of an anthropomorphic (Alderson Rando) phantom rotating at patient position during irradiation with two superposed electron beams. (Right side) Depth dose curve measured in the rotating phantom along the line shown on the film shown in the left side of the figure.

this dependence. Another possibility to produce a more homogeneous profile may be a placement of the Perspex screen at a position closer to the patient where a larger amount of the divergent electrons scattered in the screen would remain within the field of interest. This possibility was not used in this work because due to the size of the screen a larger distance was needed to provide full covering of the patient.

The described superposition technique can provide treatments with a dose homogeneity of ±4% (standard deviation, with single values up to −6/+10%) to the majority of the skin on the trunk of the patient. Larger deviations are found at the extremities and at parts of the body with a smaller diameter such as the head and neck. These overdoses are larger than the variation of the profile of the overlaid static fields at the respective positions. The higher doses at head and neck can be explained by the fact that these body regions have smaller diameters than the rump. Therefore, any surface element here will rotate slower than skin on the phantom trunk, and therefore be prone to the maximum of the beam profile for a longer time and thus receive a higher dose. A smaller effect has been theoretically calculated and measured by Podgorsak et al.[18] who reports a dose increase around 4.8% at the surface of a rotating cylinder of 15 cm diameter in comparison to a 30 cm cylinder irradiated at a distance of 285 cm from the electron source. Müller-Sievers et al.[15] report dose variations of ±10% (standard deviation ±8%) measured around the circumference of a rotating Alderson phantom at height of the umbilicus. They also assign the dose increase to the radius of curvature of the surface. However, their setup contains an additional aperture (made of 2 cm of PMMA pus 3 mm) of Al placed close to the front of the phantom. This material will act as a source of scatter radiation at short distance which can lead to enhanced distance dependence and other effects influencing the dose.

An additional cause for the dose variation seen in our measurements at the arms may be that the patient's extremities lie eccentric to the rotation axis, and therefore receive a higher dose when they are closer to the beam source, and vice versa. The result of this effect for the patient is difficult to predict since his position (and also the orientation of the skin towards the accelerator) will vary both during irradiation and from fraction to fraction. In sum, it is expected that part of the dose variation will average out.

The depth dose characteristics of the electron beam provide that the complete skin will receive at least 80% of the prescribed dose and deeper lying organs are effectively spared. The X-ray background of 1.2% measured here is higher than the 0.7% measured by Platoni et al.[16] with an ionization chamber for a similar field set-up, however, in a stationary acrylic phantom. Kim et al.[22] report 2.5% X-ray contamination measured with film and TLD in a rotating phantom with a setup which in many aspects is similar to ours, however, uses a single beam of electrons flattened by a lead filter which by itself will cause an additional X-ray background. Gerbi et al.[19] report 2–2.7% X-rays in a superposition of several electron beam arcs at shorter distance measured with an ionization chamber and films in a phantom rotated to 6 discrete positions, and Müller-Sievers et al.[15] measured 6% X-rays with films in the rotating Alderson phantom with the arrangement described above containing an additional aperture. Concerning film dosimetry one must acknowledge that the measurement of small doses as used in this work is very sensitive to correct background subtraction and therefore may have a large uncertainty.

5. Conclusions

The described technique provides a good dose uniformity within ±10% to the majority of the patient's skin. The higher doses at head, neck and extremities appear to be unavoidable. The overdoses lie well below the tolerance dose of the skin[10] (TD 5/5 (100 cm^2) = 50 Gy for telangiectasia, 55 Gy for necrosis or ulceration), so that for prescribed doses of 30–36 Gy, and in small skin areas they are clinically acceptable. However, close clinical monitoring of these regions is advised. To improve dose homogeneity, larger electron fields would be helpful, and possibly also a placement of the Perspex beam degrader immediately in front of the patient. The amount of X-ray background in TSEI treatments typically lies in the region of few per cent of therapy dose, however depends strongly on the treatment setup.

Financial disclosure

No funding or affiliation to disclose.

Conflict of interest statement

None declared.

REFERENCES

1. Hoppe RT, Fuks Z, Bagshaw MA. The rationale for curative radiotherapy in Mycosis fungoides. *Int J Radiat Oncol Biol Phys* 1977;**2**:843–51.
2. Kirova YM, Piedbois Y, Haddad E, Levy E, Calitchi E, Marinello G, et al. Radiotherapy in the management of mycosis fungoides: indications, results, prognosis. *Radiother Oncol* 1999;**51**:147–51.
3. Ysebaert L, Truc G, Dalac S, Lambert D, Petrella T, Barillot I, et al. Ultimate results of radiation therapy for T1-T2 mycosis fungoides (including reirradiation). *Int J Radiat Oncol Biol Phys* 2004;**58**:1128–34.
4. Whittacker SJ, Foss FM. Efficacy and tolerability of currently available therapies for the mycosis fungoides and Sézary syndrome variants of cutaneous T-cell lymphoma. *Cancer Treat Rev* 2007;**33**:146–60.
5. Harrison C, Young J, Navi D, Riaz N, Lingala B, Kim Y, et al. Revisiting low-dose total skin electron beam therapy in Mycosis Fungoides. *Int J Radiat Oncol Biol Phys* 2011;**81**:e651–7.
6. Lindahl LM, Kamstrup MR, Petersen PM, Wirén J, Fenger-Grøn M, Gniadecki R, et al. Total skin electron beam therapy for cutaneaous T-cell lymphoma: A nationwide cohort study from Denmark. *Acta Oncol* 2011;**20**:1199–205.
7. Nisce LZ, Safa B, Poussin-Rosillo H. Once Weekly Total and Subtotal Skin Electron Beam Therapy for Kaposi's Sarcoma. *Cancer* 1981;**47**:640–4.
8. Funk A, Hensley F, Krempien R, Neuhof D, Van Kampen M, Treiber M, et al. Palliative total skin electron beam therapy (TSEBT) for advanced cutaneaous T-cell lymphoma. *Eur J Dermatol* 2008;**18**:308–12.
9. Hauswald H, Zwicker F, Rochet N, Uhl M, Hensley F, Debus J, et al. Total skin electron beam therapy as palliative treatment

for cutaneous manifestations of advanced, therapy-refractory cutaneous lymphoma and leukemia. *Radiat Oncol* 2012;7:118, http://dx.doi.org/10.1186/1748-717X-7-118.
10. Emami B, Lyman J, Brown A, Coia L, Goitein M, et al. Tolerance of normal tissue to therapeutic irradiation. *Int J Radiat Oncol Biol Phys* 1991;**21**:109–22.
11. Karzmark CJ. Large-field superficial electron therapy with linear accelerators. *Br J Radiol* 1963;**37**:302–5.
12. Karzmark CJ, Anderson J, Buffa A, Fessenden P, Khan F, Svensson G, et al. Total skin electron therapy: technique and dosimetry. *AAPM report no. 23* New York: American Institute of Physics; 1987.
13. Holt JG, Perry DJ. Some physical considerations in whole skin electron beam therapy. *Med Phys* 1982;**9**:769–76.
14. Müller-Sievers K, Schäffler D, Kober B, Wöllgens P. Zur Dosismessung am rotierenden Phantom bei Elektronen-Abstandsbestrahlung. *Strahlenther Oncol* 1988;**164**:484–8.
15. Müller-Sievers K, Ertan E, Kober B. Dosimetry of rotational partial-skin electron irradiation. *Radiother Oncol* 2001;**58**:187–92.
16. Platoni K, Diamantopoulos S, Panayiotakis G, Kouloulias V, Pantelakos P, Kelekis N, et al. First application of total skin electron beam irradiation in Greece: setup, measurements and dosimetry. *Phys Med* 2012;**28**:174–82.
17. Williams PC, Hunter RD, Jackson SM. Whole body electron therapy in mycosis fungoides—a successful translational technique achieved by modification of an established linear accelerator. *Br J Radiol* 1979;**52**:302–7.
18. Podgorsak EB, Pla C, Pla M, Lefebvre PY, Heese R. Physical aspects of total skin electron irradiation. *Med Phys* 1982;**10**:159–68.
19. Gerbi BJ, Khan F, Deibel C, Kim TH. Total skin electron arc irradiation using a reclined patient position. *Int J Radiat Oncol Biol Phys* 1989;**17**:397–404.
20. Van der Merve DG. Total skin electron therapy: a technique which can be implemented on a conventional electron linear accelerator. *Int J Radiat Oncol Biol Phys* 1993;**27**:391–6.
21. Antolak JA, Hogstrom KR. Multiple scattering theory for total skin electron beam design. *Med Phys* 1998;**25**:851–9.
22. Kim TH, Podgorsak EB. Clinical aspects of a rotational total skin electron irradiation. *Br J Radiol* 1984;**47**:501–6.